Ecological Indicators 102 (2019) 118–130

Contents lists available at ScienceDirect

Ecological Indicators

journal homepage: www.elsevier.com/locate/ecolind

Original Articles

Can the watershed non-point source phosphorus flux amount be reflected by lake sediment?

Chen Lin[a,d,*], Changchun Huang[b,*], Ronghua Ma[a], Yuxin Ma[c]

[a] Key Laboratory of Watershed Geographic Sciences, Institute of Geography and Limnology, Chinese Academy Sciences, Nanjing 210008, China
[b] Jiangsu Center for Collaborative Innovation in Geographical Information Resource Development and Application, Nanjing Normal University, Nanjing 210023, China
[c] Sydney Institute of Agriculture, School of Life & Environmental Sciences, The University of Sydney, NSW 2006, Australia
[d] State Key Laboratory of Soil and Sustainable Agriculture, Institute of Soil Science, Chinese Academy of Sciences, Nanjing 210008, China

ARTICLE INFO

Keywords:
Watershed
Non-point source pollution
Lake Sediment
Land use/cover change (LUCC)

ABSTRACT

An understanding of the quantitative relationship between watershed non-point source (NPS) pollution and lake nutrient enrichment is essential for the environmental management of water bodies. However, a lack of data availability and integration limit our understanding of this relationship. The most critical bottlenecks are the lack of adequate support for watershed-lake integrated data, a lack of data of the nutrient loading from watersheds into a lake as NPS, and the long-term time series data of lake nutrient concentrations. Since lake sediment is the ultimate destination of watershed nutrients, this study aimed to reveal the relationship between watershed phosphorus (P) concentrations that are transported into lakes and lake P concentrations by using inlet sediments as an indicator. Three typical sub-basins within Hongze Lake, China were selected as the study site, and 30-year dataset was calculated using the technology integration of remote sensing, sediment chemical analysis and SWAT model assessment. It can be concluded that, first, the Mineral-P (Min-P) accounted for nearly 65% of the watershed Total P (TP) loss, which varied over different basins and temporal periods. Second, the relationship between watershed P loss into lakes and sediment P concentrations represented obvious variation among different basins, sediment depths and P states. With respect to different basins, the highest correlation appeared in Basin 1, which had a R^2 value of 0.65 for Min-P. With respect to different P states, the Inorganic-P (IP) showed a closer relationship between watershed and lake P than Organic-P (OP), and the correlation coefficient (r) was higher than 0.6 in Basin 1 and Basin 3 for IP. In addition, the calcium-phosphorus ratio (Ca-P), which is largely sourced from watershed rock detritus by eroded runoff, played the most critical role among different Min-P states in the relatively ideal relationship of IP. With respect to different sediment depths, a stratification phenomenon existed in Basin 2 and Basin 3, which differed at specific depths. In particular, the ideal relationship only existed within the 7 cm depth from the bottom in basin 2, and this value expands to 10 cm for basin 3. This diversity was influenced by the integration roles from external and endogenous sources. All the findings indicated that lake surface sediment can be used as a proxy to represent NPS P loading under specific conditions. The relationship between watershed P loss and lake sediment P concentration was largely decided by land use/cover change (LUCC), meteorological conditions, and lake resuspension.

1. Introduction

Phosphorus (P) is an essential element for crop growth and a primary nutrient involved in the eutrophication of aquatic ecosystems (Norton et al., 2012). Recently, soil P loss via watershed agricultural non-point source (NPS) pollution has been recognized as a severe threat to the aquatic environment, and a significant portion (80%) of lost P exists in particulate form (Evanylo et al., 2008; Castoldi et al., 2009). Therefore, watershed NPS P pollution governance could have significant benefits for lake ecology and environmental protection. Determining the relationship between NPS P loads and lake nutrient enrichment becomes a priority (Ouyang et al., 2013).

Currently, watershed non-point source (NPS) phosphorus (P) pollution monitoring and lake P concentration trend studies are two independent and separate research subjects. With respect to NPS P load monitoring, numerous physically-based (e.g., SWAT, ANSWERS, and

* Corresponding authors at: Key Laboratory of Watershed Geographic Sciences, Institute of Geography and Limnology, Chinese Academy Sciences, Nanjing 210008, China (C. Lin).
E-mail address: clin@niglas.ac.cn (C. Lin).

https://doi.org/10.1016/j.ecolind.2019.02.031
Received 26 August 2018; Received in revised form 17 January 2019; Accepted 16 February 2019

AGNPS) and empirical models (e.g., RUSLE, and PLOAD) have been developed in recent decades and have been widely used to evaluate spatial P pollution loads under specific environmental conditions (Bechmann et al., 2009; Blair and Aller, 2012; Laurent and Ruelland, 2011). The Soil and Water Assessment Tool (SWAT), the most widely used physically based model, is frequently used to estimate basin-wide sediment and nutrient fluxes for regional planning (Neitsch et al., 2011; Arnold et al., 2012; Gassman et al., 2014). The SWAT model considers several management practices, e.g., considering land use change, pollutant transport and reservoirs (Vigiak et al., 2017); therefore, several important sources of sediments, such as gully erosion or landslide movements can be explicitly assessed by SWAT (de Vente et al., 2013).

Regular and periodic lake monitoring and laboratory measurements are critical for the acquisition of lake P concentration data. Long-term monitoring has been advantageous for researching lake environments in some European countries (Mogan et al., 2012). In China, research started relatively late, compared with European and American countries. Lake monitoring in China has rapidly increased since the 1990s, and research has largely been carried out in typical eutrophic lakes including Taihu Lake, Chao Lake and Hongze Lake (Zhu et al., 2003). For instance, the total Phosphorus (TP) concentrations in a severely eutrophic section of Hongze Lake ranged from 0.10 to 0.38 mg L^{-1}, whereas values were less than 0.05 mg L^{-1} in the less polluted lake center (You et al., 2015). However, it should be noted that data publicity and availability have remained at relatively low levels. The lack of data records is considered the most important factor limiting the development of monitoring and analysis for the lake water environment. The lack of existing monitoring data limits our ability to assess the relationship between NPS P loads and lake P concentrations over long time periods (Yang et al., 2012). Nevertheless, lake sediment is the ultimate destination of watershed nutrients and can, therefore, be an ideal supplement and substitute for lake P data (Guildford and Hecky, 2000; Morgan et al., 2012; Ahmed et al., 2012).

For the acquisition of lake P concentration data, regular and periodic lake monitoring and laboratory measurements are critical. Long-term monitoring has been conducted in some European countries that are advantageous for lake environment research (Mogan et al., 2012). In China, the research has begun relatively late, compared with European and American countries. Lake monitoring in China has been rapidly developed since the 1990s, and research has largely been carried out in typical eutrophic lakes including Taihu Lake, Chao Lake and Hongze Lake (Zhu et al., 2003). For instance, the TP concentrations in the severely eutrophic section of Hongze Lake ranged from 0.10 to 0.38 mg L^{-1}, whereas values were less than 0.05 mg L^{-1} in the less polluted lake centre (You et al., 2015). However, it should be noted that data publicity and availability have remained at a relatively low level. The lack of data records is considered the most important factor limiting the development of lake water environment monitoring and analysis. It suggests that the existing monitoring data cannot meet the requirements of the scale consistency between data of NPS P loads and lake P change in a long temporal sequence (Yang et al., 2012). Nevertheless, the lake sediment can be designated as an ideal supplement and substitution for lake P data acquisition (Guildford and Hecky, 2000; Morgan et al., 2012).

Previous research has observed a relationship between TP concentrations in lake sediment and lake water. A study found that the TP concentration in the surface sediment column (0–15 cm) varied from 0.60 to 0.98 g kg^{-1} in the river–lake edge area of Hongze Lake. This value was not only larger than that at the lake center but also larger than those in the lake sediments of some pollution-free inland lakes in Europe, including Loch Leven and Lake Windermere (He et al., 2005; Xue et al., 2007; Rothwell et al., 2010). These results showed that the spatial pattern of TP concentration in sediments was consistent with those in lake water. Nevertheless, sediment TP concentrations were larger than those of the lake water. Moreover, the spatial variations of TP concentration in lake sediment and lake water were primarily due to the drastic land-use changes and massive amount of watershed nutrient losses (Erol and Randhir, 2013).

Therefore, the watershed NPS P assessment and Lake P monitoring are the two critical issues for the research of watershed nutrient transportation and are also important for watershed-lake integrated management (Lin et al., 2016). However, studies focusing on lake water and those focusing on watershed nutrients have been relatively separate from each other, which can be considered as the most critical technical bottleneck for watershed-lake integrated research (Amiri et al., 2012; Yang et al., 2012). A quantitative analysis of the influence of NPS P outputs on lake TP concentration is urgent. Such analysis could be largely dependent upon the long temporal series data acquisition of watershed NPS P modelling and lake sediment P analysis.

Several typical sub-basins within the Hongze Lake basin were selected as the study site. Agricultural non-point source (ANPS) pollution is acknowledged as the most important major exogenous source contributor to lake nutrient enrichment because the selected basins are largely dominated by traditional agriculture and have been affected by drastic land use/cover changes (LUCC) in the last 30 years (Zhou et al., 2013). The objectives of this study were: i) To assess the temporal and spatial variation tendencies in watershed NPS P loads and lake sediment P concentrations, based on SWAT model and sediment analysis, where the organic and inorganic P are introduced respectively; and ii) To explore the relationship between watershed P outputs and lake sediment P concentrations within different basins and discuss the suitability of using lake sediments to reflect the watershed NPS P flux.

2. Materials and methods

2.1. Study site

Hongze Lake is located in Huaian and Suqian Cites, Jiangsu Province, China, and the lake belongs to the Huaihe River Basin. The monsoon climate leads to abundant rainfall in the watershed, with an average annual precipitation of 1145 mm in the study area. The main rainfall season is from June to September. The major soil types are yellow brown soil and paddy soil, where TP concentrations range from 0.2 to 1.3 g/kg and soil organic matter (SOM) ranges from 5 to 30 g/kg.

The watershed is an important production base of traditional agriculture and animal husbandry, with arable land accounting for more than 65% of the whole watershed. For this case, ANPS is regarded as the main watershed pollution source, causing lake quality degradation. Some research has indicated that soil phosphorus (TP) loss into lakes from the surrounding watershed is largely sourced from NPS pollution and that the proportion exceeded 80% (You et al., 2015; Yang, 2009). Nutrient enrichment has resulted in acute fluctuations in the water quality of Hongze Lake, degrading from grade II to grade III and IV over approximately thirty years (Li and Pu, 2003).

Importantly, the rapid development of socioeconomic standing and drastic land-use management has taken place since 1990, and unbalanced patterns and spatial diversity features have also been noticeably exhibited, within different regions or sub-basins. Therefore, three sub-basins, which represented three typical land use/cover change patterns, were selected in this study. The first is the watershed of Gaosong River tributary (basin 1), representing a rapid urbanization area. According to the land use dataset developed by Data Center for Geography and Limnology Science, Chinese Academy of Science, CAS (the more specific information of the land use dataset was showed in Table. 1), the proportion of construction land has increased 22.12% during the last 30 yrs; ii) the second is the watershed of Bian River tributary (basin 2), representing a wetland reserve area and located in the transition zone from the land to the lake; iii) the third is the watershed of Weiqiao River tributary (basin 3), representing an area with different land use types including construction land, arable land, forestland, bare land and water.

Table 1
Overview of data for sediment load modelling and P flux simulation.

Data	Year	Resolution	Source	Description
Digital elevation model	–	90 m	Shuttle Radar Topography Mission (SRTM)[a]	Acquired from http://strm.csi.cgiar.org (Version 4.1), The length factor and slope factor were extracted from the DEM
Land use	1990, 1995, 2000, 2005 2010, 2015	30 m	Data Center for Geography and Limnology Science, Chinese Academy of Science, CAS	The spatial data of land use/cover change(LUCC) were produced by Data Center for Geography and Limnology Science, Chinese Academy of Science, the Landsat Thematic Mapper (TM) satellite images covering the study area were downloaded from U. S. Geological Survey (http://earthexplorer.usge.gov) and used to extract the major land use types, including original forest, planted forest, agricultural land, construction land, wetland and unutilized land. The data production work was processed every five years, and the validation of interpretation results was conducted by fieldwork (63 samples were located in the study site); the data accuracy could reach 85%. Currently, the data can be downloaded from http://lake.geodata.cn/.
Soil properties	Three stages: Stage 1: 1987–2004: Stage 2: 2005–2011: Stage 3: 2012–2015	Stage 1: soil types Stage 2: 1 km grids Stage 3: Field samples	Stage 1: Harmonized Word Soil Database Stage 2: The second geochemical survey data in Jiangsu Province (processed from 2005 to2007) Stage 3: Field sampling and measurements (processed in 2013 and 2014)	(1) First stage: the background values of soil organic matter (SOM), Total Phosphorus (TP), and particle composition were assigned based on different soil types, information for which was acquired from the Harmonized Word Soil Database (HWSD) with 1:100000 resolutions (http://www.fao.org). (2) Second stage: The spatial maps of SOM and particle composition were developed based on data from the second geochemical survey in Jiangsu Province, which was conducted from 2005 to 2007. The 1 km grid equidistant sample data were acquired in 2008, and the spatial interpolation was processed using ArcGIS. (3) Third stage: The surface soil samples (0–10 cm depth) were collected from Oct. 2013 to Feb. 2014 in different sub-basins, immediately after the freezing period and before the plowing season. The sampling sites were 150 m to 200 m apart (using a global positioning system) to ensure spatial uniformity. The samples covered three critical land-use patterns, including forest, arable land and orchard land. At each site, soils were sampled 9 times within a radius of 20 m from the plot centre and were then mixed into a single sample. A total of 25 points were sampled in each sub-watershed.
Weather data	1988–2010	$0.2^{\circ} \times 0.2^{\circ}$	Climate Forecast System Reanalysis (CFRS) http://globalweather.tamu.edu	the runoff data and Temperatures from 1988 were collected over 10-day periods, and the data were processed by monthly averaged and spatial interpolation.

Table 2
Sensitivity parameters for water discharge and sediment export in this study.

	Parameter	Definition	Range
Discharge	CN_2	Initial SCS runoff curve number for moisture condition II	35–98
	ALPHA_BF	Base flow alpha factor (1/days).	0–1
	GW_DELAY	The delay time of groundwater	0–500
	GWQMN	Threshold depth of water in the shallow aquifer required for return flow to occur (mm H_2O).	0–5000
	CANMX	Maximum canopy storage (mm H_2O).	0–100
	ESCO	Soil evaporation compensation factor.	0–1
	SOL_AWC	Available water capacity of the soil layer (mm H2O/mm soil).	0–1
	SURLAG	Surface runoff lag coefficient	0.05–24
	RCHRG_DP	Deep aquifer percolation fraction.	0–1
	CH_K_2	Effective hydraulic conductivity in main channel alluvium (mm/hr).	−0.01 to 500
	EPCO	Plant uptake compensation factor.	0–1
	CH_N_2	Manning's "n" value for the main channel.	−0.01 to 0.3
	REVAPMN	Threshold depth of water in the shallow aquifer for "revap" or percolation to the deep aquifer to occur (mm H_2O).	0–500
	SFTMP	Snowfall temperature (°C).	−20 to 20
	GW_REVAP	Groundwater "revap" coefficient.	0.02–0.2
	SOL_K	Saturated hydraulic conductivity (mm/hr).	0–2000
Sediment	USLE_P	USLE equation support practice factor.	0–1
	SLSUBBSN	Average slope length (m).	10–150
	HRU_SLP	Average slope steepness (m/m).	0–1
	RSDCO	Residue decomposition coefficient.	0.02–0.1
	SPCON	Linear parameter for calculating the maximum amount of sediment that can be restrained during channel sediment routing.	0.0001–0.01
	SPEXP	Exponent parameter for calculating sediment restrained in channel sediment routing	1–1.5
	CH_ERODMO	A value of 0.0 indicates a non-erosive channel while a value of 1.0 indicates no resistance to erosion.	0–1
	CH_COV1	Channel erodibility factor.	−0.05 to 0.6
	CH_COV2	Channel cover factor.	−0.01 to 1
	BIOMIX	Biological mixing efficiency.	0–1

2.2. Simulation of sediment and amounts of watershed P loss into lake in temporal

2.2.1. Hydrological module and sediment erosion in SWAT model

The SWAT model uses the SCS curve number procedure (USDA Soil Conservation Service, 1972) and the Green & Ampt infiltration method to estimate surface runoff volume for each Hydrological Response Unit (HRU) (Green and Ampt, 1911). At the same time, a modified rational method is used to calculate the peak runoff rate, which is an important indicator of the erosive power of a storm and is used to predict sediment loss. In this model, Manning's equation is used to define the rate and velocity of flow. The water is routed through the channel network using two kinds of kinematic wave models: the variable storage routing method (Williams, 1969) and Muskingum River routing method (Cunge 1969). Details of kinematic wave model can be seen in Saleh and Arnold (2000).

$$Q_{surf} = (R_{day} - -I_a)^2/(R_{day} - -I_a + S) \quad (1)$$

Where Q_{surf} is accumulated runoff or excess rainfall (mm); R_{day} is the rainfall depth on a day (mm); I_a is the initial losses (mm), including ground fill, plant retention and infiltration before the runoff; S is the retention parameter (mm).

The SWAT model uses the Modified Universal Soil Loss Equation (MUSLE) (Williams, 1975) to calculate erosion caused by rainfall and runoff. MUSLE is a modified version of Universal Soil Loss Equation (USLE) developed by Wischmeier and Smith (1987). Rainfall energy factor is used to predict average annual gross erosion, which is replaced by runoff factor in MUSLE because rainfall energy factor can only represent energy used in detachment while runoff factor represents energy used in detaching and transporting sediment. In addition, other factors used in MUSLE include soil erodibility factor, cover and management factor, support practice factor, topographic factor, and coarse fragment factor.

$$A_i = R_i \times K_i \times LS_i \times C_i \times P_i \quad (2)$$

where Ai is the soil erosion modulus (kg·km^{-2}·yr^{-1}), R_i is the rainfall-runoff erosivity factor (MJ mm· (ha h yr)$^{-1}$); K_i is the soil erodibility factor (Mg h MJ2^{-1}mm^{-1}); LS_i is the slope length and steepness factor; C_i is the cover management factor; and PL_i is the conservation support practice factor which is based on land uses (Ferro and Porto, 1999; Capolongo et al., 2008).

2.2.2. SWAT input data

The ArcSWAT interface for SWAT version 2012 is an extension of ArcGIS/ArcMap to compile the SWAT input files. The basic datasets required to construct the model include topography, land use, soil, and weather data. The details of the data source and description are given in Table 1. To meet the requirements of the entire temporal scale from 1990s to 2015, the land use data of six periods (1990/1995/2000/2005/2010/2015) were used to simulate sediment of different periods, respectively.

2.2.3. Sensitivity analysis of parameter

LH-OAT (Wei et al., 2009) global parameter sensitivity analysis was used to analyze the sensitivity of the model. LH-OAT assumed that each parameter is divided into N spaces, then a random sample of these sample spaces (the probability of being drawn in each space is 1/N) was selected. All parameters were combined randomly, and the model results were analyzed using multi-parameter linear regression or correlation analysis method after running the model run N times.

$$S = \frac{\Delta R}{\Delta P_i} \times \frac{P_i}{R} \quad (3)$$

Where S is the sensitivity index, R is the model outputs, P_i is the model outputs factor, ΔP_i is the variation of model influence factor (parameter), ΔR is the variation of the model outputs. Sensitivity parameters and their specific conditions were described in Table. 2

2.2.4. Calibration and validation of SWAT

The SUFI-2(Abbaspour et al., 2007) procedure in SWAT-CUP (Abbaspour, 2011) software was used to calibrate and validate the model. The deterministic coefficient (R2) and the Nash-Sutcliffe coefficient (NSE) were used to evaluate the model.

$$\mathrm{Ens} = 1 - \left(\sum_{i=1}^{n} (Y_{obs,i} - Y_{sim,i})^2 / \sum_{i=1}^{n} (Y_{obs,i} - Y_{obs,av})^2 \right)$$

Table 3
Classification of the SWAT model performance.

Classes	R2	NSE
Very good	$R^2 = 1.00$	$0.75 < NSE \leq 1.00$
Good	$0.80 \leq R^2 < 1.00$	$0.65 < NSE \leq 0.75$
Satisfactory	$0.60 \leq R^2 < 0.80$	$0.40 < NSE \leq 0.65$
Unsatisfactory	$R^2 < 0.60$	$NSE \leq 0.40$

$$R^2 = \left(\frac{\sum_{i=1}^{n} (Y_{obs,i} - Y_{obs,av})(Y_{sim,i} - Y_{sim,av})}{\sqrt{\sum_{i=1}^{n} (Y_{obs,i} - Y_{obs,av})^2} \sqrt{\sum_{i=1}^{n} (Y_{sim,i} - Y_{sim,av})^2}} \right)^2 \quad (4)$$

The Nash–Sutcliffe coefficient (*Ens*) was used to assess the performance of the model in this study. Where $Y_{obs,i}$ is the measured value, $Y_{sim,i}$ is the simulation value, $Y_{obs,av}$ is the measured average value, and n is the number of observations. *Ens* ranges from $-\infty$ to 1. The model evaluation criteria area presented in Table 3 (Moriasi et al., 2015;Santhi et al., 2010).

The monitoring data from 2006 to 2011 were collected from Yaowei hydrological station located in Sihong County. The model calibration and validation were conducted based on the land-use map of 2010. Therefore, the calibration period was selected from 2006 to 2009, and the validation period was from 2010 to 2011.

The model validation results in Fig. 2 indicate that the simulation results of water discharge and sediment export are highly related with their respective observed values in the entire calibration period (Fig. 2), in which the values of NSE and R^2 for calibration and validation were greater than 0.77. This result implied that the SWAT model can be used to effectively simulate the water discharge and sediment export in Hongze Lake Basin. Therefore, the Mineral-P (Min-P) and OP (Organic-P) loss amounts into lake from 1987 to 2015 can be simulated based on the hydrological models that are established by the land-use data of their corresponding periods.

2.3. TP concentrations in lake sediment

In order to ensure the minimum disturbance of the sediment–water interface, the sediment locations were selected in lake inlets about 50 m distance to the corresponding watershed outlets. Moreover, four columns were collected for each watershed for the purpose of comprehensive sample coverage, and then the four columns were mixed into one sediment core, representing the corresponding sub-basin. Therefore, a total of twelve columns were collected using a gravity-type corer in situ in March 2015 (Fig. 1), and finally three 25 cm long and 4 cm diameter sediment cores were generated for laboratory measurements.

The sediment cores were pre-treated in the laboratory of School of Geographic Science, Nanjing Normal University. The sediment cores were sliced into 1 cm segments from top to bottom, and the sliced layers were sealed in polyethylene bags and immediately transported to the laboratory. The samples were air-dried in a lyophilizer, grounded with a mortar and pestle (XPM-120x3, China), and passed through a 100-meshnylon sieve.

The specific activity concentrations of the sliced cores were dated using the activity of an ^{210}Pb ($^{210}Pb_{ex}$) radiometric technique based on the method suggested by Mizugakia et al. (2006), and the radiometric measurements were operated with gamma spectrometer (ORTEC., USA). The deposition rate of the sediment cores was determined by the following algorithms, which is made up by specific activity concentrations and buried depth of sediment:

$$D_R = \frac{D_S}{t} = \frac{\lambda D_S}{\ln \frac{I_0}{I_S}}$$

$$I_s = I_0 e^{-\lambda t} \quad (5)$$

$$t = \frac{\ln \frac{I_0}{I_S}}{\lambda}$$

where $D_R$represents the deposition rate, and the D_S represents the sediment burial depth, the t is the deposition time, the I_0 is the initial specific activity concentrations of ^{210}Pb, and I_s means the specific activity concentrations of ^{210}Pb after t years, and the specific historical hydrology and meteorology data (flooding and strong rainfall) were used to correct the geochronology estimated by $^{210}Pb_{ex}$. Finally, the particular years that corresponding to each sliced cores can be acquired by the calculation results of deposition rates. The results showed that the deposition rate of No. 1, No.2 and No. 3 cores were 0.40 cm/a, 0.413 cm/a and 0.42 cm/a, respectively. This result is consistent with previous studies, which showed that the deposition rate within Hongze Lake is approximately 0.40 cm/a (He et al., 2005).

In addition, the TP concentrations of each slice of three sediment cores were measured with inductively coupled plasma (ICP) methods at the State Key Laboratory of Soil and Sustainable Agriculture, Institute of Soil Science, Chinese Academy of Sciences. The Standard Measurement Test (SMT) method was applied to acquire the chemical speciation of phosphorus including organic (OP) and inorganic (IP) phosphorus, constituting mainly of iron (Fe-P), aluminum (Al-P), and calcium-bound phosphors (Ca-P). The SMT is a sediment phosphorus fractionation method harmonized and validated in the frame of the 'standards, measurements and testing programme' of the European Commission (Ruban et al., 1999) The Al-P, Fe-P, OP, Ca-P were extracted by 0.5 mmol/L NH4F, 1 h, 0.1 mmol/L NaOH, 0.5 mmol/L NaOH, 16 h and 1.0 mmol/L NaAc-HAc, 6 h consecutively. The SMT protocol has also been tested on three sediments (calcareous, siliceous, organic-rich) and the results reported were considered satisfactory (Wang et al., 2013).

3. Results

3.1. Simulation of watershed P amount loss into lake.

The amount of phosphorus transported into the aquatic system, including OP and Min-P, were assessed by the SWAT model. Fig. 3 compares the concentration loss of different P states, within three sub-basins in the past 30 yrs. In general, the three sub-basins represent similar spatial tendencies, in which a notable fluctuation trend can be found within all the three basins. In particular, four phases can be summarized as follows:

i) The first phase ranged from 1985 to 1991; during this period Hongze Lake experienced severe NPS P pollution, as well as increasing P deposits. The peaks within basin 1 and basin 2 appeared in 1987 and 1989, respectively. The average TP concentrations exceeded 2 t/a, even reaching 9.63 t/a within basin 3 in 1991. ii) The second phase ranged from 1992 to 1995, with a notable downward trend found within all the three basins, especially in basin 1 and basin 2, where the TP amounts were almost less than 0.6 t/a. iii) The third phase, ranging from 1996 to 2007, deposition rates of TP into the lake experienced fluctuating increasing trend. The peaks appeared in some discontinuous years such as 1998, 2000, 2003 and 2006. Interestingly, the TP concentrations decreased significantly in the other years. iv) The fourth phase ranged from 2008 to 2014. A steady and continuous decreasing trend can be found in this phase. The TP loss into the lake remained approximately 0.6 t/a, 0.7 t/a and 4.1 t/a for the three basins since 2011.

Different basins also presented notable differences for NPS P loss into the lake. In general, the TP loss into the lake within basin 3 showed significantly higher values than the other two basins, where values rarely exceeded 2 t/a in most of the years. Conversely, the TP amount within basin 3 even approached 10 t/a in certain years such as 1991, 1998, 2003 and 2006. The proportions of Min-P (IP) were higher than OP in the three basins. For instance, the average Min-P amount within basin 1 in the whole temporal sequence was 0.55 t/a, compared to

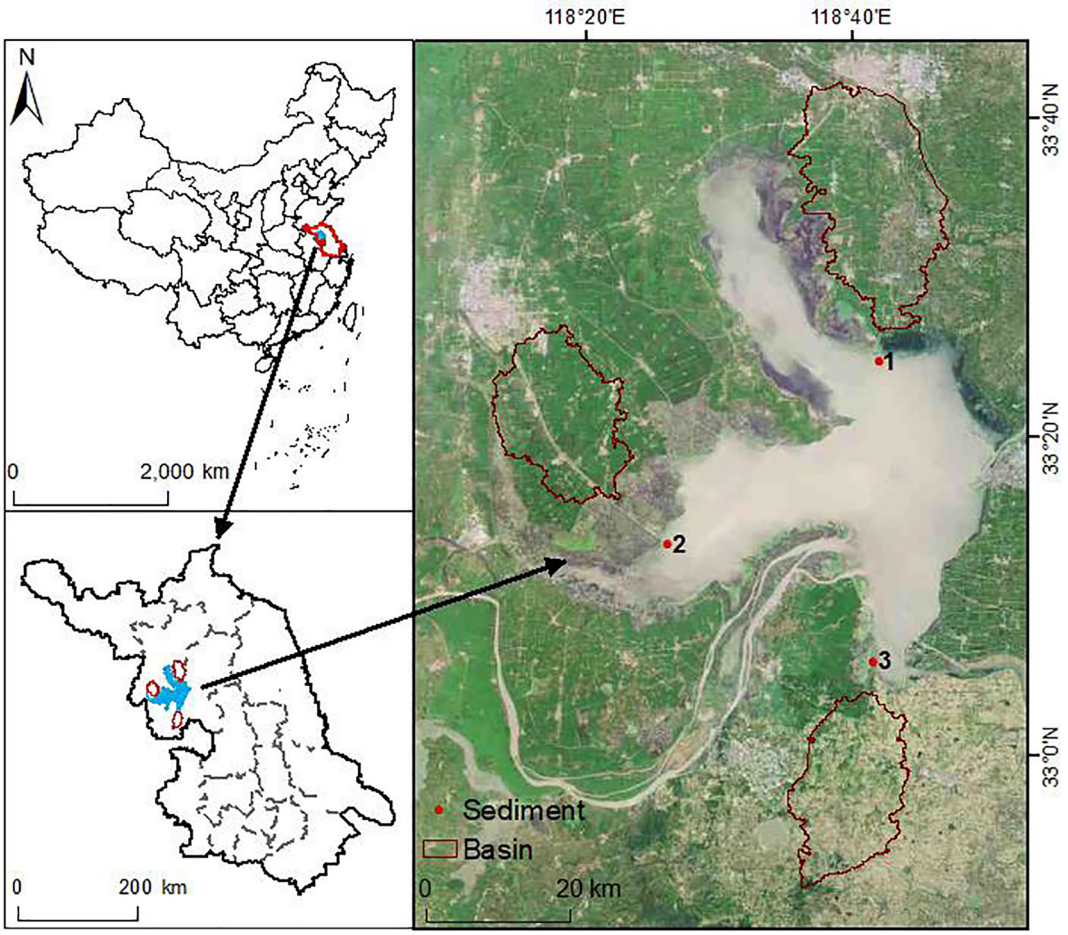

Fig. 1. The study sites.

0.36 t/a for OP. A similar trend can be found in basin 2 and basin 3, simultaneously, where the average Min-P amount was nearly 1.5 times the OP amount in general.

3.2. Lake P concentration trends over the last 30 years

According to the ^{210}Pb radiometric measurements, the deposition rate of Hongze Lake remained at approximately 0.40 cm/a; this indicates that each 1 cm slice can represent 2–3 years historically, and the geochronology of the sediment core (0–15 cm) can meet the requirements of the temporal scale in this study, ranging from 1987 to 2015. IP concentrations are consistently higher than OP in all sediments regardless of location or depth (Fig. 4). IP concentrations largely varied from 300 to 500 mg/kg while the OP concentrations rarely exceeded 100 mg/kg.

Importantly, the IP concentrations also represented more notable variations in trends throughout the whole temporal series (Fig. 4). Several extreme high values for IP appeared alternately over a relative short period, mostly in basin 1. Conversely, OP concentrations are more consistent over the entire period, with the most stable trend-line in

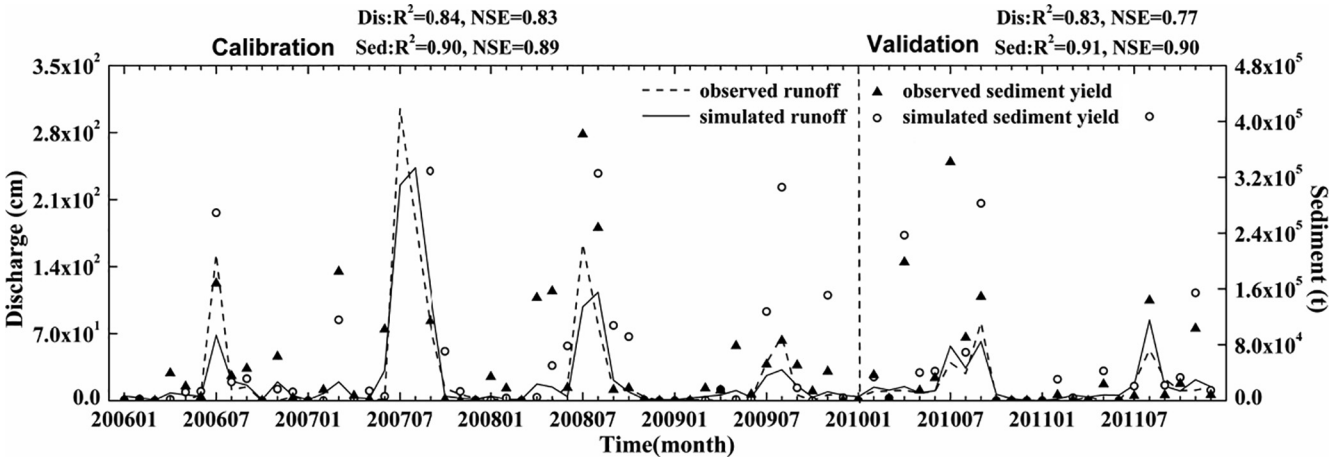

Fig.2. Simulated and observed water discharge and sediment export in Yaowei station during the calibration period and validation period.

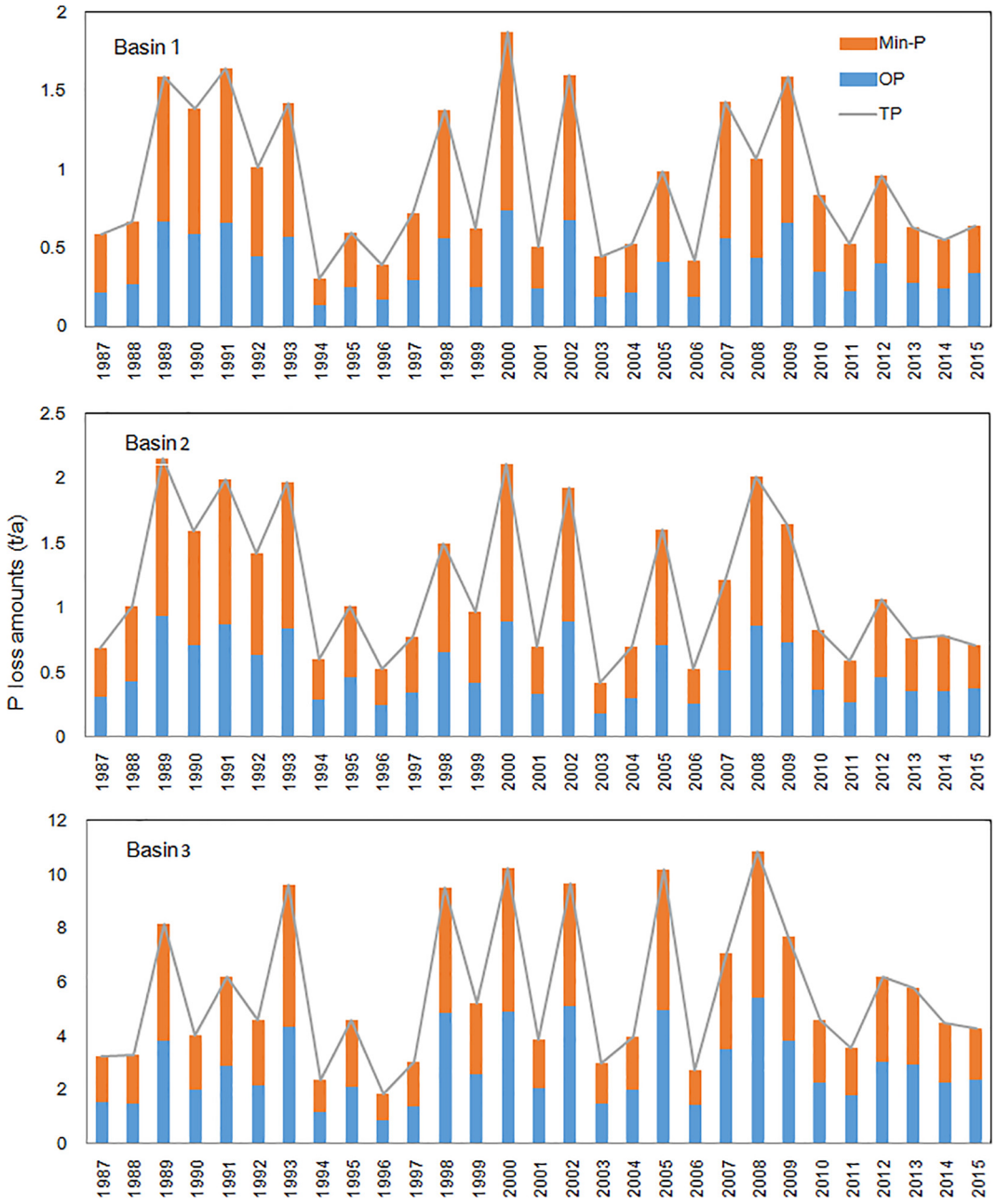

Fig. 3. The multi-states P loss amounts into lake within different basins.

basin 2. Nevertheless, the OP concentrations have increased gradually since 2001 in basin 3, where the maximum value reached 108.65 mg/kg in 2009. The opposite trend is found in basin 1, where the OP concentrations have decreased to some extent since 2003, and the lowest concentration of 40 mg/kg corresponds to 2005.

3.3. Relationship between sediment P and watershed NPS P loads

The relationship between the amount of watershed P lost into lakes and sediment P concentration in the entire temporal sequence was calculated based on different P states including OP, IP and TP in different basins. In addition, previous studies have shown that the IP accounted for nearly 80%-90% of watershed Min-P composition (Beck and Sanchez, 1996; Sun et al., 2011), meaning watershed Min-P loss can be related to lake sediment IP concentration. A two-year interval was defined and averaged from 1987 to 2015, with 15 available items generated for each basin. The basic statistical data of the correlation degree between watershed NPS P loads and lake sediment P concentrations in three basins are shown in Table 4, in which the different P states such as TP, Organic-P and Inorganic-P were contained. In addition, 'integrated' means that all the available data items were considered together, without the classification of different basins. Further detailed information is given in scatter plots, and the OP and IP are represented (Fig. 5).

In general, the basin 1 provides the greatest correlation coefficient between the amount of watershed P loss into lakes and lake sediment P concentrations under all P states, particularly with respect to IP (r = 0.77). IP always has a much higher correlation coefficient when compared with OP. Specifically, the r for IP also achieved 0.6 for basin 3, yet the correlation degree of OP was below 0.2.

The correlation between lake TP and watershed TP was relatively poor both in basin 2 and basin 3. In particular, the r value for basin 2 was approximately 0.2, degrading the general correlation degree that considered all the basins together (Table 4). It is also notable that the r

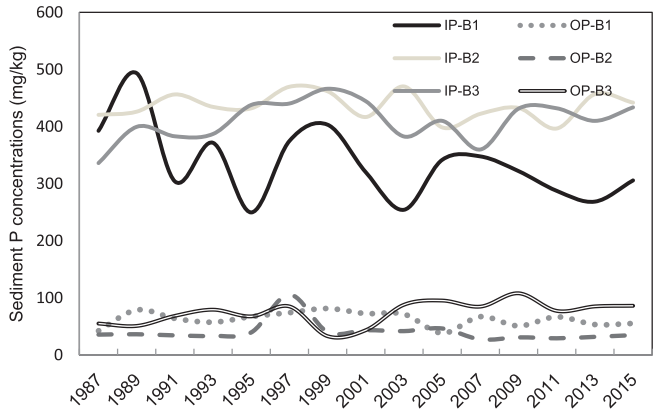

Fig. 4. The tendency of sediment IP and OP concentrations in the entire temporal scales within different basins (eg: IP-B1 represented the IP concentrations with Basin 1, as well as OP-B1 represented the OP concentrations with Basin 1).

value was still close to 0.5 when the plots for different basins were integrated and passed the test for $p < 0.01$. These findings showed that there are strong linkages between watershed and lake sediment P under certain circumstances. A deep analysis and discussion are needed.

4. Discussion

The lake sediment P has rarely been linked with watershed P outputs in the previous studies, due to the lack of long-term data support (Hoffmann et al., 2009; Ouyang et al., 2013). Several related studies have indicated that watershed NPS P pollution leads to lake quality degradations through watershed nutrients delivery from inflowing rivers into lakes (Ahearn et al., 2005). This implies that lake sediment can be an ideal repository and suitable recorder of watershed NPS P representation. Moreover, these issues also provide a useful theoretical basis for this study, which aimed to link NPS P outputs and lake P accumulation. From the correlation results shown in Table 4, we believed that some interesting issues needed a deeper discussion and analysis. Firstly, why did the ideal correlation can be observed in the relationship between watershed Min-P loss and lake IP? Secondly, why did such relationship in basin 1 seem to be the best among different basins? And why did such relationship in the basin 2 was the poorest? For this case, the various sediment P states, as well as different sediment layers can be proposed as suitable explanations.

4.1. The impact of different sediment P fractions

The correlation coefficients of IP were much better than that of OP (Table 4), and the only exception existed in basin 2 (the poor relationship can be found for IP and OP simultaneously). Therefore, the influence mechanisms of IP between watershed and lake sediment should be focused on basin 1 and basin 3.

Different P fractions are complicated in lake sediment P. Ca-P and Fe/Al-P are the most important P states of sediment IP (Andrieux, 1997; Ruban et al., 2001; Wang et al., 2008). Previous research has indicated that these two states accounted for nearly 90% of IP in Hongze Lake (Wang et al., 2011), which is consistent with the results of this study. In addition, this study further indicated that the Ca-P concentrations accounted for nearly 60% of the sediment IP, which proportions are greater than Fe/Al-P in a majority of sediment slices in Hongze Lake (Fig. 6). For instance, the sediment Ca-P concentrations of basin 1 and basin 3 are consistently around 170–240 mg/kg for different sediment slices, while the Fe/Al-P concentrations seldom exceeded 110 mg/kg. Moreover, it is noteworthy that the activity and susceptibility of the Ca-P and Fe/Al-P are significantly different (Hisashi, 1983). This suggests that the Ca-P and Fe/Al-P concentrations in different sediment slices and different basins need to be considered separately, and correlated with watershed IP outputs in the corresponding years represented by that the sediment layer. A total of fifteen data items can be achieved in each basin, to cover the entire temporal sequence (Fig. 7).

Importantly, the fitting effect of sediment Ca-P and watershed Min-P outputs were much better than that of Fe/Al-P, and most were prominently represented in basin 1 (R^2 up to 0.7). Therefore, an interesting inference can be concluded, which was rarely mentioned in previous studies: the Ca-P is the most important sediment inert P component in the relationship between watershed Min-P and sediment IP. Ca-P is difficult to combine with other lake suspended substances (Camargo and Alonso, 2006; Burley et al., 2001), and the lake sediment Ca-P is mainly sourced from watershed rock detritus eroded during runoff, as well as the decomposition of lake algae and microbial residues (Tang et al., 2017). Hongze Lake is located in the midstream of Huai River, one of the seven large rivers in China, and has two specific features that differentiate it from other large eutrophic lakes such as Taihu and Chaohu Lakes. These are more frequent surface water exchange and relatively high suspended particulate matter (SPM) concentrations, which can reach up to 100 mg/L (Cao et al., 2018). Both of these features directly contribute to the increasing turbidity of Hongze Lake and further inhibit the lake algae growth and microbial reproduction (Zhu et al., 2004). This suggests that the endogenous sources are not the primary source of sediment Ca-P. Instead, exogenous sources, such as watershed outputs, contributed the greatest to lake sediment Ca-P concentrations. In actual fact, the Hongze Lake basin is dominated by agricultural land that is processed with large quantities of urea and calcium superphosphate fertilizer (Andrieuxf, 1997). The higher watershed soil Ca-P concentrations are associated with greater Min-P loss into lakes, and most likely existed in Ca-P state in lake sediment. This explains the positive relationship between the watershed Min-P and sediment Ca-P within Basin 1 and Basin 3.

The Fe/Al-P showed a relatively poor relationship to watershed Min-P outputs, compared with Ca-P, with an $R^2 < 0.2$. The most likely explanation is that Fe/Al-P has high activity, and is, therefore, likely to combine with other lake substances such as suspended solids and aquatic vegetation under certain nutrient concentrations and hydrological conditions (Young and Ross, 2001; Rubak et al., 2013). The distribution observed in Fig. 5 supports this assertion. The Fe/Al-P

Table 4
Statistical data of the relationship between watershed NPS P loads and lake sediment TP concentrations in three basins.

Indicators[#]	TP		Organic-P		Inorganic-P	
	correlation coefficient (r)	RMSE[@]	correlation coefficient (r)	RMSE[@]	correlation coefficient (r)	RMSE[@]
Basin 1	0.69**	0.22	0.46**	0.12	0.77**	1.01
Basin 2	0.22	0.93	0.14	1.72	0.30	0.89
Basin 3	0.32*	0.87	0.19	0.33	0.60**	0.67
Integrated	0.47*	1.22	0.40*	0.98	0.58**	1.01

*: $p < 0.05$; **: $p < 0.01$
[@] : Root Mean Squared Error.
[#] : the relationship between watershed loss amount into lake (TP/Organic-P/Inorganic-P) and the lake sediment concentrations (TP/Organic-P/Inorganic-P).

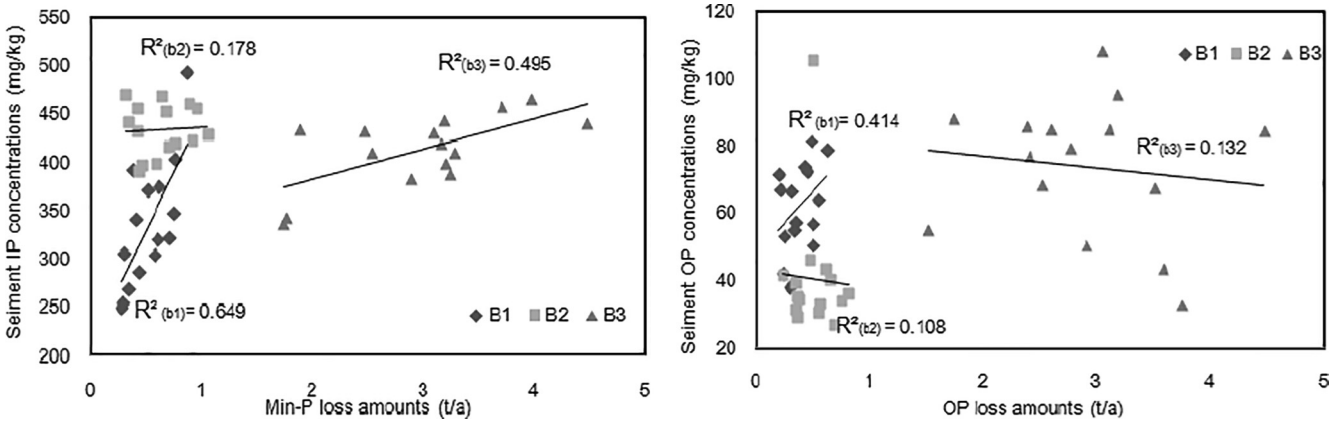

Fig. 5. The scatter plots of watershed P loss amounts into lake and sediment P concentrations for the whole temporal scales (eg: $R^2_{(B1/B2/B3)}$ represented the R^2 value for the plots belonging to each basin).

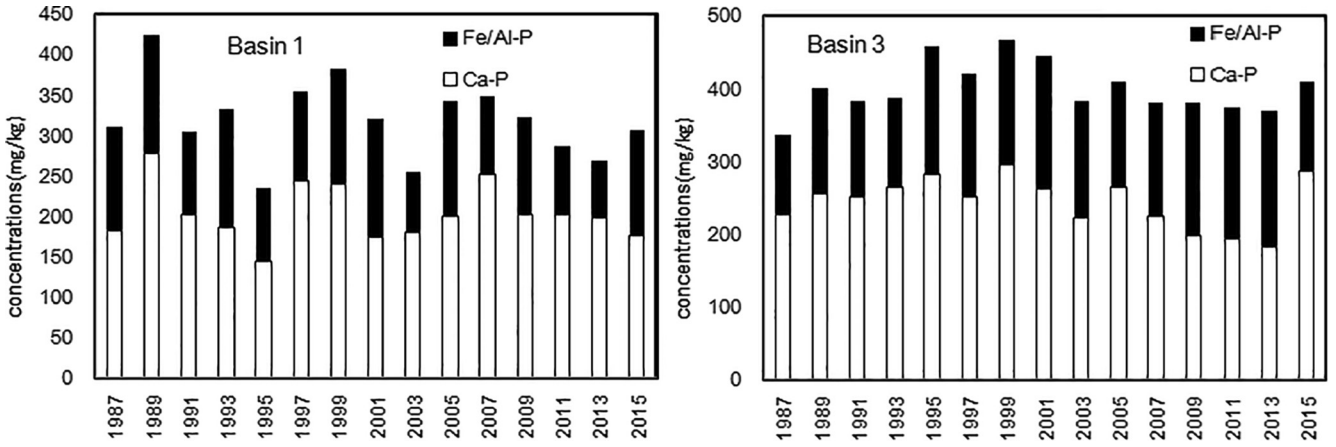

Fig. 6. The sediment Ca-P and Fe/Al-P concentrations within basin 1 and basin 3.

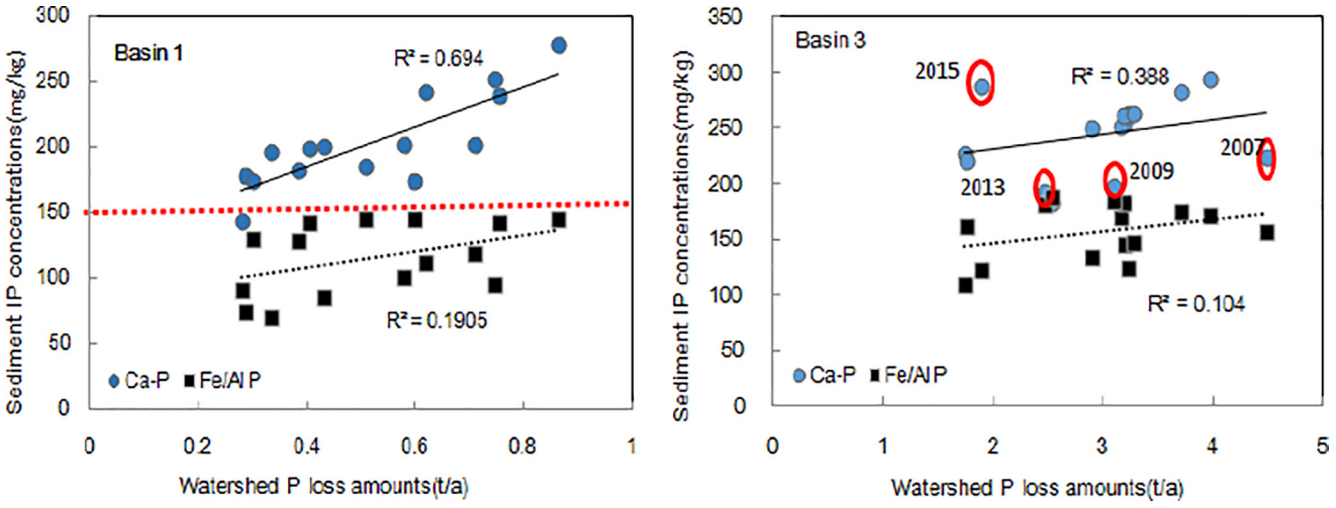

Fig. 7. The scatter plots of watershed Ca-P and Fe/Al - P loss amounts and sediment P concentrations within basin 1 and basin 3.

concentrations of basin 1 did not maintain the increasing trend with more Min-P loss when the sediment Fe/Al-P concentrations reached 150 mg/kg. Similarly, basin 3 had shown a weaker relationship than basin 1. This can be ascribed to the data from 2007, 2009, 2011 and 2015, which were furthest from the trend line. Interestingly, basin 3 possessed higher Fe/Al-P concentrations than basin 1, particularly from 2007 to 2013, in which the Fe/Al-P concentrations reached 200 mg/kg, and the proportions of Fe/Al-P in IP are also approaching that of Ca-P (Fig. 6). Therefore, the high Fe/Al-P concentrations did not associate with the good relationship between watershed Min-P and sediment Fe/Al-P. A similar explanation can be also applied to the OP, which also had high activity and was poorly related to watershed P outputs.

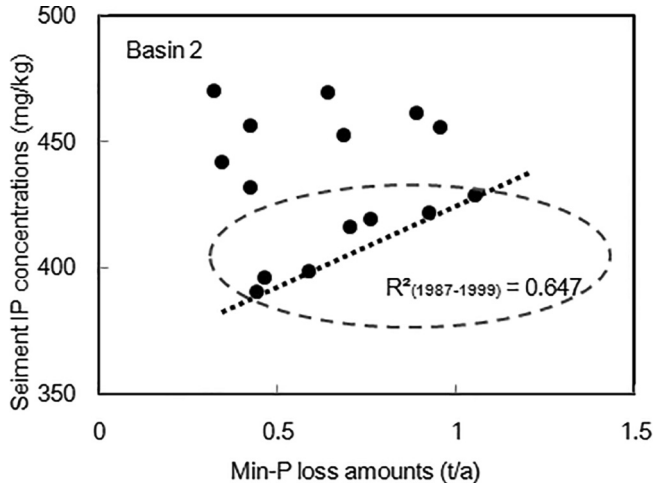

Fig. 8. The scatter plots of watershed Min-P loss amounts and sediment IP concentrations within basin 2.

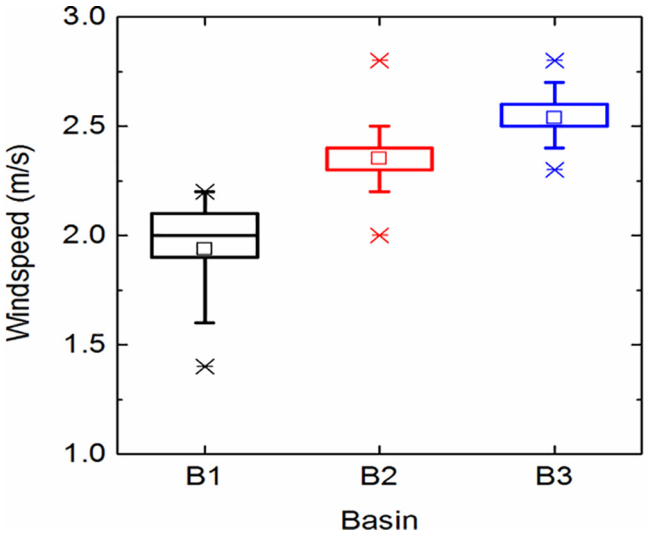

Fig. 9. The box charts of the wind speed data in the entire temporal scales within different basins.

4.2. The sediment stratification phenomenon occurred by the integrated roles from internal and external sources

The last section indicated that a better relationship was observed in the slices close to the sediment bottom for basin 3, which means the stratification phenomenon existed in the relationships between watershed and lake P. It should be noted that this phenomenon can also be found in basin 2, despite the generally poor results showed in Table 4. In specific, the relative ideal positive correlation degree between watershed min-P loss amounts and sediment IP concentrations could be achieved when only seven plots were taken into consideration ($R^2 = 0.65$), and these plots represent the successive scales from 1987 to 1999 (Fig. 8). However, the correlation coefficient rapidly decreased when the other plots were taken into consideration. This stratification phenomenon was similar to that of basin 3, indicating that two phases need to be considered respectively throughout the entire temporal series. The explanation can be given both from endogenous and external sources.

With respect to the endogenous source, the notable disparity between the two temporal phases can be interpreted in terms of sediment resuspension, which is used to describe the substance exchange between the lake sediment surface and overlying water under extreme meteorological conditions (Wan et al., 2010). Lake resuspension usually involves the top 5–10 cm of the sediment surface in the mid-lower Yangtze Lakes, including Taihu Lake, Chaohu Lake, Yangcheng Lake and Hongze Lake (Qin et al., 2003; Taube et al., 2018). This finding can partly explain the reason for the poor relationship within the sediment core slices near the sediment surface of basin 2 and basin 3. Lake resuspension involves the suspension of particulate matter that has accumulated on the sediment surface under the influence of wind-wave disturbances (Schallenberg and Burns, 2004), which indicates that meteorological information, especially that of wind-speed, plays an important role in the assessment of lake resuspension. Three national meteorological stations are located in three sub-basins, and the yearly wind speed data were acquired from the China Meteorological Data Sharing Service Platform (http://data.cma.cn/), which covered the entire temporal scale (1987–2015). The annual average wind speed (2.0 m/s) appears to be lower in basin 1 than in basin 2 and basin 3, in which the yearly averaged wind speeds exceeded 2.2 m/s, and the peak wind speed was 2.8 m/s (Fig. 9). Therefore, the remarkable lake resuspension led by meteorological factors can partly explain the stratification phenomenon for basin 2 and basin 3. In addition, the only difference between the two basins is the specific depth of the lake resuspension. The resuspension depth of Basin 3 was approximately the top 5 cm, which represented the time since 2007. The depth of resuspension in basin 2 expanded into 9 cm from the sediment surface, representing the time since 1999. This difference further revealed that the influences of external sources outside the watershed cannot be neglected.

Anthropogenic activities play an important role in watershed nutrient delivery and deposition for lake sediment. The land use/cover change (LUCC) is an important indicator of human disturbance (Petrosell et al., 2014) because human activities which affect the land surface directly can lead to nutrient loss (Maanan et al., 2014; Ouyang et al., 2016). It is acknowledged that arable land, forestland, and in-built land are likely major sources of NPS P pollution and transportation (Ahearn et al., 2005). Therefore, the spatial distributions of these typical land-use patterns in the three sub-basins are presented in Fig. 10.

The most drastic land use change can be found in basin 1. The conversion from forest to arable land, as well as the conversion of arable land to in-built land, occurred throughout the temporal scale. Nevertheless, the rate of change varied largely within different temporal intervals. For instance, despite the substantial urbanization that has occurred since 1990, the rate of urbanization unexpectedly slowed between 2010 and 2015. Moreover, basin 1 has been undergoing land consolidation and rehabilitation since 2010 (Hu et al., 2012), in which several land consolidation and reclamation projects took place, for the control of agricultural pollution and improvement of the environmental (Cao et al., 2017). Therefore, the notable fluctuation features of NPS P loss into the lake (Fig. 3), especially the decreasing tendency for IP loss within basin 1 since 2010, can be explained by the reduction in the rate of urbanization and more effective arable land protection.

In contrast, relatively stable and uniform land use types can be found in basins 2 and 3. These stable LUCC features were inconsistent with the notable fluctuations of NPS P loss tendency. Although there was a decrease in arable land which corresponds to the increase in in-built land area, the magnitude of this land use change was much lower than that in basin 1. For instance, the arable land area in basin 3 remained approximately 155 km^2 to 162 km^2, and the in-built land has ranged from 22 km^2 to 30 km^2 since 1990. However, an increasing trend of in-built land has occurred between 2010 and 2015, with a nearly 9 km^2 increase during the 5-year period. The increase in impermeable land surface area and continuous agricultural chemical fertilization in these areas have impacted surface infiltration and resulted in the increased loss of P from watershed soil. In addition, higher P loss occurred in basin 3 largely due to the undulating topography in the southern part of the basin, which experiences higher velocity stream flows and sediment loading.

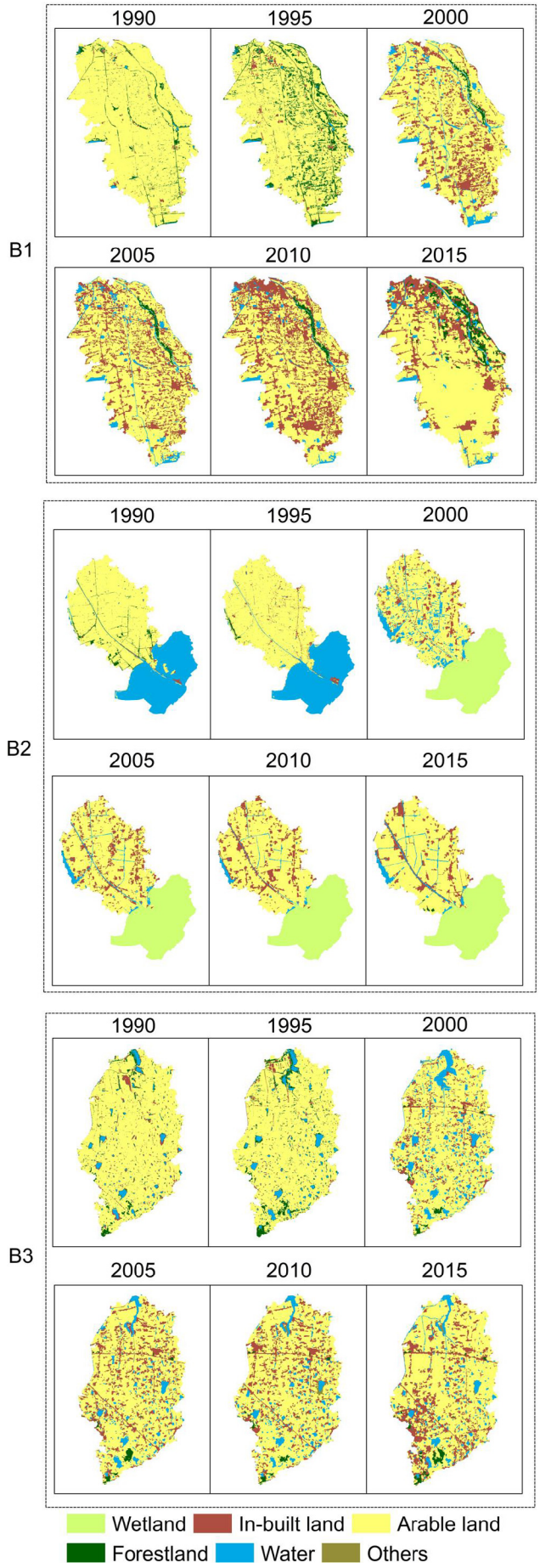

Fig. 10. The spatial features of different land use patterns in the entire temporal scales (the year of 1990, 1995, 2000, 2005, 2010 and 2015 were given).

The wetland distributed in basin 2 provides reasonable explanations for the poor relationship between watershed P and lake sediment P. Wetlands are described as "the kidney of the earth", for their role in the removal of pollutants and nutrients, including COD, $NH4+$-N and TP, in watersheds, (Maltais-Landry et al., 2009; Naylor et al., 2003). Interestingly, a wetland region can be found easily in the critical transition zone between the watershed area of basin 2 and lake aquatic system since 2000 (Fig. 10). This region is actually the Wetland Nature Reserve of Hongze Lake (WNR), a constructed wetland, developed in 1999 (Li and Pu, 2003). The majority of constructed wetlands have been successfully developed for treating domestic, industrial, and agricultural wastewater, especially for lake water purification and eutrophication inhibition. This may explain the weak relationship between watershed P loss and lake sediment P concentrations within basin 2, as well as the shallower sediment depth for NPS pollution representation, due to the wetland provide effective retention capability for N and P pollutants in watershed drainage that is favorable for inhibiting lake eutrophication.

5. Conclusions

This study aims to integrate the watershed P outputs and lake P concentrations, using lake sediment as an important indicative indicator. The study developed a 30-year temporal sequence in three typical sub-basins within Hongze Lake, with quantitative multi-state watershed P outputs, as well as lake sediment P concentrations from 1987 to 2015. Most importantly, we found that the relationship between watershed P loss into lakes and sediment P concentrations represented obvious variation among different basins, sediment depths and P states. The results can be concluded that:

First, the watershed TP outputs by ANPS showed a notable fluctuation trend with time. TP composition is proportionally Min-P rather than OP; nevertheless, the amount of watershed P output to lakes represented diversity among different watersheds, which is largely determined by the temporal features of Min-P.

Second, watershed Min-P loss amounts were well linked with lake inorganic-P concentrations, particularly Ca-P from eroded rock detritus, during the whole time within different basins.

Thirdly, Basin 1 revealed a relatively ideal relationship between watershed P outputs and lake P concentration. However, such a relationship in the other two basins represented a notable stratification phenomenon, which differed at specific depths. The notable disparity in temporal scale can be effectively interpreted in terms of the integration role of extraneous sources from watershed and the role of endogenous sources from lake resuspension.

Therefore, the sediment can be designated as an ideal indicator for the watershed NPS P pollution representation, especially for IP. Importantly, the top sediment layer may experience lake resuspension and result in the degradation of the relationship between watershed P outputs and lake P accumulations. This study provides an important basis for the linkage between watershed, streamway and lake ecosystem, and introduces a feasible predictive tool to simplify the NPS P, especially the IP pollution representation assessment. In addition, the methods used in this research are also needed to further study other areas to determine whether this linkage between watersheds and lakes can be universally applied.

Acknowledgments

This work was funded by The National Natural Science Foundation of China (Grant No. 41671284) and Research Fund of Key Laboratory of Coastal Zone Exploitation and Protection, Ministry of Land and

Resource (2015CZEPK01). Data were supported by Scientific Data Sharing Platform for Lake and Watershed, Nanjing Institute of Geography and Limnology, Chinese Academy of Sciences.

References

Abbaspour K.C: SWAT-CUP. 2012. SWAT Calibration and Uncertainty Programs – A User Manual, 2011.

Abbaspour, K.C., Yang, J., Maximov, I., Siber, R., Bogner, K., Mieleitner, J., Zobrist, J., Srinivasan, R., 2007. Modeling hydrology and water quality in the pre-alpine/alpine Thur watershed using SWAT. J. Hydrol. 333, 413–430.

Ahearn, D.S., Sheibley, R.W., Dahlgren, R.A., Anderson, M., Johnson, J., Tate, K.W., 2005. Land use and land cover influence on water quality in the last free flowing river draining the western Sierra Nevada, California. J. Hydrol. 313 (3–4), 234–247.

Ahmed, F., Bibi, H., Asaeda, T., Mitchell, C.P.J., Ishiga, H., Fukushima, T., 2012. Elemental composition of sediments in Lake Jinzai, Japan: assessment of sources and pollution. Environ. Monitoring Assess. 184, 4383–4396.

Amiri, B.J., Sudheer, K.P., Fohrer, N., 2012. Linkage between in-stream total phosphorus and land cover in Chugoku district Japan: an ANN approach. J. Hydrol. Hydromech. 60, 33–44.

Andrieuxf, A.A., 1997. Two-year survey of phosphorus speciation in the sediments of the Bay of Seine (France). Cont. Shelf Res. 17 (10), 1229–1245.

Arnold, J.G., Kiniry, J.R., Srinivasan, R., Williams, J.R., Haney, E.B., Neitsch, S.L., 2012. Soil and Water Assessment Tool Input/Output documentation Version 2012. Texas Water Resources Institute Technical report 436. Texas A&M University System College Station, Texas, U.S. http://swat.tamu.edu/documentation/2012-io/, accessed. 17.12.2014.

Bechmann, M., Stalnacke, P., Kvoerno, S., Eggestad, H.O., Oygarden, L., 2009. Integrated tool for risk assessment in agricultural management of soil erosion and losses of phosphorus and nitrogen. Sci. Total Environ. 407 (2), 749–759.

Beck, A., Sanchez, P.A., 1996. Soil phosphorus movement and budget after 13 years of fertilized cultivation in the Amazon basin. Plant Soil 184, 23–31.

Blair, N.E., Aller, R.C., 2012. The fate of terrestrial organic carbon in the marine environment. Annual review of marine science. Ann. Rev. Marine Sci. 4 (1), 401–423. https://doi.org/10.1146/annurev-marine-120709-142717.

Burley, K.L., Prepas, E.E., Chambers, P.A., 2001. Phosphorus release from sediments in hardwater eutrophic lakes: the effects of redox-sensitive and -insensitive chemical treatments. Freshw. Biol. 46 (8), 1061–1074.

Camargo, J.A., Alonso, A., 2006. Ecological and toxicological effects of inorganic nitrogen pollution in aquatic ecosystems: a global assessment. Environ. Int. 32 (6), 831–849.

Cao, Y.T., She, D.L., Liu, B., Xu, C.L., Ding, J.H., Sui, X.Y., 2017. Research on land consolidation comprehensive benefit evaluation of Jiangsu Province. China Rural Water Hydropower. 1, 27–32 (in Chinese).

Cao, Z.G., Duan, H.T., Shen, M., Ma, R., Xue, K., 2018. Using VIIRS/NPP and MODIS/Aqua data to provide a continuous record of suspended particulate matter in a highly turbid inland lake. Int. J. Appl. Earth Obs. Geoinf. 64, 256–265.

Capolongo, D., Diodato, N., Mannaerts, C.M., Piccarreta, M., Strobl, R.O., 2008. Analyzing temporal changes in climate erosivity using a simplified rainfall erosivity model in Basilicata (southern Italy). J. Hydrol. 356, 119–130.

Castoldi, N., Bechini, L., Stein, A., 2009. Evaluation of the spatial uncertainty of agro-ecological assessments at the regional scale: the phosphorus indicator in northern Italy. Ecol. Ind. 9 (5), 902–912.

Cunge, J.A., 1969. On the subject of a flood propagation method (Muskingum method). J. Hydraulics Res. 7 (2), 205–230.

de Vente, J., Poesen, J., Verstraeten, G., Govers, G., Vanmaercke, M., Van Rompaey, A., Arabkhedri, M., Boix-Fayos, C., 2013. Predicting soil erosion and sediment yield at regional scales: where do we stand? Earth Sci. Rev. 127, 16–29.

Erol, A., Randhir, T.O., 2013. Watershed ecosystem modeling of land-use impacts on water quality. Ecol. Model. 270, 54–63.

Evanylo, G., Sherony, C., Spargo, J., Starner, D., Brosius, M., Haering, K., 2008. Soil and water environmental effects of fertilizer-, manure-, and compost-based fertility practices in an organic vegetable cropping system. Agric. Ecosyst. Environ. 127 (1–2), 50–58.

Ferro, V., Porto, P., 1999. A comparative study of rainfall erosivity estimation for southern Italy and southeastern Australia. Int. Assoc. Sci. Hydrol. Bull. 44, 3–24.

Gassman, P.W., Sadeghi, A.M., Srinivasan, R., 2014. Applications of the SWAT model special section: overview and insights. J. Environ. Quality 43, 1–8.

Green, W.H., Ampt, G.A., 1911. Studies on Soil Physics: Part I — the flow of air and water through soils. J. Agric. Sci. 4 (1), 11–24.

Guildford, S.J., Hecky, R.E., 2000. Total nitrogen, total phosphorus, and nutrient limitation in lakes and oceans: is there a common relationship? Limnol. Oceanogr. 45 (6), 1213–1223.

He, H.C., Ding, H.Y., Zhang, Z.K., Shi, X.D., Li, S.H., Mao, L.J., 2005. Grain-size characteristics and Their Environmental Significance of Hongze Lake Sedmients. Scientia Geographical Sinica. 25 (5), 590–596.

Hisashi, J., 1983. Fractionation of phosphorus and releasable fraction in sediment mud of Osaka Bay. Bull. Jap. Soc. Sci. Fish 49 (3), 447–454.

Hoffmann, C.C., Kjaergaard, C., Uusi-Kamppa, J., Hansen, H., Kronvang, B., 2009. Phosphorus retention in riparian buffers: review of their efficiency. J. Environ. Qual. 38 (5), 1942–1955.

Hu, Y.C., Zheng, X.Q., Xu, J.Y., Zheng, Y.M., 2012. Regional difference for newly increased cultivated land area through land consolidation in China. Trans. CSAE 28 (2), 1–6.

Laurent, A., Ruelland, D., 2011. Assessing impacts of alternative land use and agricultural practices on nitrate pollution at the catchment scale. J. Hydrol. 409 (1–2), 440–450.

Lin, C., Wu, Z.P., Ma, R.H., Su, Z.H., 2016. Detection of sensitive soil properties related to non-point phosphoruspollution by integrated models of SEDD and PLOAD. Ecol. Ind. 60, 483–494.

Maanan, M., Ruiz-Fernandez, A.C., Maanan, M., Fattal, P., Zourarah, B., Sahabi, M., 2014. A long-term record of land use change impacts on sediments in Oualidia lagoon, Morocco. Int. J. Sediment Res. 29, 1–10.

Maltais-Landry, G., Maranger, R., Brisson, J., 2009. Effect of artificial aeration and macrophyte species on nitrogen cycling and gas flux in constructed wetlands. Ecol. Eng. 35 (2), 221–229.

Morgan, B., Rate, A.W., Burton, E.D., 2012. Water chemistry and nutrient release during the resuspension of FeS-rich sediments in a eutrophic estuarine system. Sci. Total Environ. 432 (15), 47–56.

Moriasi, D.N., Gitau, M.W., Pai, N., Daggupati, P., 2015. Hydrologic and water quality models: performance measures and evaluation criteria. Trans. ASABE 58, 1763–1785.

Naylor, S., Brisson, J., Labelle, M.A., Drizo, A., Comeau, Y., 2003. Treatment of freshwater fish farm effluent using constructed wetlands: the role of plants and substrate. Water Sci. Technol. 48 (5), 215–222.

Neitsch, S.L., Arnold, J.G., Kiniry, J.R., Williams, J.R., 2011. Soil and Water Assessment tool - theoretical documentation. Texas Water Resources Institute Technical report 406. University System College Station, Texas, U.S, Texas A&M.

Norton, L., Elliott, J.A., Maberly, S.C., May, L., 2012. Using models to bridge the gap between land use and algal blooms: an example from the Loweswater catchment, UK. Environ. Modell. Softw. 36, 64–75.

Ouyang, W., Shan, Y.S., Hao, F.H., Chen, S.Y., Pu, X., Wang, M.K., 2013. The effect on soil nutrients resulting from land use transformations in a freeze-thaw agricultural ecosystem. Soil Tillage Res. 132 (8), 30–38.

Ouyang, W., Jiao, W., Li, X.M., Giubilato, E., Critto, A., 2016. Long-term agricultural non-point source pollution loading dynamics and correlation with outlet sediment geochemistry. Sci. the Total Environ. 540, 379–385.

Petrosell, A., Lenoe, A., Ripa, M.N., Recanatesi, F., 2014. Linking phosphorus export and hydrologic modeling: a case study in Central Italy. Environ. Monit. Assess. 186, 7849–7861.

Qin, B.Q., Hu, W.P., Gao, G., Luo, L.C., Zhang, J.S., 2003. Dynamic mechanism of suspended sediment and the conceptual model of endogenous release in Taihu Lake. Chin. Sci. Bull. 48 (17), 1821–1831.

Rothwell, J.J., Dise, N.B., Taylor, K.G., Allott, T.E.H., Scholefield, P., Davies, H., Neal, C., 2010. A spatial and seasonal assessment of river water chemistry across North West England. Sci. Total Environ. 408, 841–855.

Ruban, V., Lopez-Sanchez, J.F., Pardo, P., Rauret, G., Muntau, H., Quevauviller, P., 2001. Development of a harmonised phosphorus extraction procedure and certification of a sediment reference material. J. Environ. Monit. 3, 121–125.

Rubak, G.H., Kristensen, K., Olesen, S.E., Ostergaard, H.S., Heckrath, G., 2013. Phosphorus accumulation and spatial distribution in agricultural soils in Denmark. Geoderma 209–210, 241–250.

Saleh, A., Arnold, J.G., 2000. Applicati on of SWAT for the upper North Bosque River Watershed. Trans. ASAE 43 (5), 1077–1087.

Santhi, C., Arnold, J.G., Williams, J.R., Dugas, W.A., Srinivasan, R., Hauck, L.M., 2010. Validation of the SWAT model on a large river basin with point and nonpoint sources, Jawra. J. Am. Water Resour. Assoc. 37, 1169–1188.

Schallenberg, M., Burns, C.W., 2004. Effects of sediment resuspension on phytoplankton production: Teasing apart the influences of light, nutrients and algal entrainment. Freshw. Biol. 49 (2), 143–159.

Sun, G.F., Jin, J.Y., Shi, Y.L., 2011. Research advance on soil phosphorous forms and their availability to crops in soil. Soil and Fertilizer Sciences in China. 2, 1–9.

Tang, H.W., Zhao, H.Q., Li, Z.W., Yan, S.Y., Li, Q.X., Ji, F., Xiao, Y., 2017. Phosphorus sorption to suspended sediment in freshwater. Water Manage. 170, 231–242.

Taube, R., Ganzert, L., Grossart, H.P., Gleixner, G., Premke, K., 2018. Organic matter quality structures benthic fatty acid patterns and the abundance of fungi and bacteria in temperate lakes. Sci. Total Environ. 610, 469–481.

USDA Soil Conservation Service, 1972. National Engineering Handbook. Hydrology Section 4 (Chapters 4–10).

Vigiak, O., Malagó, A., Bouraoui, F., Vanmaercke, M., Obreja, F., Poesen, J., 2017. Modelling sediment fluxes in the Danube River Basin with SWAT. Sci. Total Environ. 599–560, 992–1012.

Wan, J., Wang, Z., Yuan, H.Z., 2010. Characteristics of phosphorus fractionated from the sediment resuspension in abrupt expansion flow experiments. J. Environ. Sci. China 22 (10), 1519–1526.

Wang, C., Zou, L.M., Wang, P.F., Lin, Z.P., 2008. Environ. Sci. 29 (5), 1303–1307.

Wang, C.Y., Zhang, Y., Li, H.L., Morrsion, R.J., 2013. Sequential extraction procedures for the determination of phosphorus forms in sediment. Limnology. 14 (2), 147–157.

Wang, Z.Q., Zhang, S.H., Xu, Z.F., 2011. Forms of Phosphorus in Sediments from Hongze Lake. Environ. Monit. Forewarning 3 (6), 40–44.

Wei, B., Guo qiang, L., Yi wei, D., Juan, X., Xiao hui, L., 2009. Parameters auto calibration with modified SWAT. Chinese J. Agrometeorol. 30 (s2), 271–275.

Williams, J.R., 1969. Flood routing with variable travel time or variable storage coefficients. Trans. ASAE 12 (1), 100–103.

Wischmeier, W.H., Smith, D.D., 1987. Predicting Rainfall Erosion Losses a Guide to Conservation Planning. US Department of Agriculture, Agricultural Handbook, Washington D C, USDA, pp. 537.

Xue, B., Yao, S.C., Wang, S.M., Xia, W.L., 2007. Enrichment of nutrients and analysis of its reason in sediment of different kinds of lakes at middle and lower Yangtze River Basin. J. Lake Sci. 27 (1), 122–127.

Yang, 2009. Researches on Characteristics and Influencing Factors of Phosphorus Loss in Runoff in the Typical Land use of Taihu Watershed. Zhejiang University Press, Zhejiang, China (in Chinese).

Yang, M., Li, X., Hu, Y.M., He, Y.Y., 2012. Assessing effects of landscape pattern on sediment yield using sediment delivery distributed model and a landscape indicator. Ecol. Ind. 22, 38–52.
You, A.J., Wu, Z.Y., Han, Z.C., Yang, J., Hua, L., 2015. Spatial and temporal distributions and variations of nutrients in the West Lake, Hangzhou, after the implementation of integrated water management program (1985–2013). J. Lake Sci. 27 (3), 371–377.
Young, E.O., Ross, D.S., 2001. Phosphate release from seasonally flooded soils. J. Environ. Qual. 30, 91–101.
Zhou, L., Xu, J.G., Sun, D.Q., Ni, T.H., 2013. Spatial Heterogeneity and classified control of agricultural non-point source pollution in Huaihe River Basin. Environ. Sci. 34 (2), 547–554.
Zhu, G.W., Qin, B.Q., Gao, G., Zhang, L., Fan, C.X., 2004. Fractionation of phosphorus in sediments and its relation with soluble phosphorus contents in shallow lakes located in the middle and lower reaches of Changjiang River, China. Acta Scientiae Circumstantiae 24 (3), 381–388.